

Accuracy and Precision Analysis of Chamber-Based Nitrous Oxide Gas Flux Estimates

Rodney T. Venterea*

Kurt A. Spokas

John M. Baker

USDA-ARS

Soil and Water Management Research Unit

1991 Upper Buford Circle

439 Borlaug Hall

St. Paul, MN 55108

Chamber-based estimates of soil-to-atmosphere nitrous oxide (N_2O) gas flux tend to underestimate actual emission rates due to inherently nonlinear time series data. In theory, this limitation can be minimized by adjusting measurement conditions to reduce nonlinearity and/or by using flux-calculation (FC) schemes that account for the so-called "chamber effect." The current study utilizes gas transport theory and stochastic analysis to evaluate accuracy and precision of N_2O flux determinations under specific soil and chamber conditions. The analysis demonstrates that measures taken to increase the absolute accuracy of flux estimates, including shorter deployment times, larger chamber heights, and nonlinear FC schemes, will also increase the variance in flux estimates to an extent that depends on errors associated with sampling techniques and analytical instrument performance. These effects, in the absence of any actual variation in fluxes, can generate coefficients of variation ranging from 3 to 70% depending on measurement conditions. It is also shown that nonlinear FC schemes are prone to generating positively skewed distributions. These effects decrease confidence in N_2O flux estimates and inhibit the detection of differences arising from experimental factors. In general, a linear FC scheme will be more likely to detect relative differences in fluxes, although less accurate in absolute terms than nonlinear schemes. The techniques described here have been codified into an accessible spreadsheet-based tool for evaluating accuracy and precision trade-offs under specific measurement conditions.

Abbreviations: CV, coefficient of variation; DT, deployment time; ECD, electron capture detector; GC, gas chromatograph; h , chamber height; HM, Hutchinson & Mosier; FC, flux-calculation; MC, Monte Carlo; Quad, quadratic; RE, relative error; WFPS, water-filled pore space.

Accelerating demand for biofuel crops and rising worldwide fertilizer consumption have elevated the importance of accurate measurement of soil N_2O emissions (Crutzen et al., 2008; Verge et al., 2007). Due to its high global warming potential relative to CO_2 , soil N_2O emissions have a large impact on the greenhouse gas budget of agro-ecosystems (Forster et al., 2007; Mosier et al., 2005; Robertson et al., 2000). However, on scales ranging from field to global, there is great uncertainty in assessing N_2O emissions. The current global estimate of agricultural N_2O emissions has an uncertainty ranging from -60 to 170% of the mean estimate (Denman et al., 2007). More than 90% of reported soil N_2O emissions data have been obtained using non-steady state chamber methods (Stehfest and Bouwman, 2006). Rochette and Eriksen-Hamel (2008) concluded that 50 to 60% of N_2O chamber data reported to date have "low or very low confidence levels" due to method inadequacies.

While studies have recommended improvements in chamber methods (e.g., Hutchinson and Livingston, 2002), there are fundamental aspects for which there are no clear guidelines. There is no consensus regarding the best method for calculating

fluxes using chamber concentration versus time data. It is well known that chamber deployment suppresses the concentration gradient at the soil-atmosphere interface. This so-called "chamber effect" results in nonlinearity in the data and an underestimation of predeployment flux by up to 40% (Livingston and Hutchinson, 1995). Some researchers attempt to minimize these errors by adjusting measurement conditions to maximize linearity. Decreasing total chamber deployment time (DT) and increasing effective chamber height (h) each tend to reduce nonlinearity. However, Livingston et al. (2006) demonstrated that even small deviations from linearity can result in relatively large errors. Others have proposed nonlinear calculation schemes (Hutchinson and Mosier, 1981; Wagner et al., 1997; Livingston et al., 2006). Venterea and Baker (2008) demonstrated that both linear and nonlinear FC models generate more accurate estimates when DT is decreased and h is increased. However, another consequence of decreasing DT and increasing h is that changes in chamber trace gas concentrations relative to initial (ambient) concentrations are reduced. Thus, the ability of N_2O analysis systems (e.g., gas chromatography) to reliably detect small changes in concentration will affect the precision of resulting flux estimates. The objective of the current study was to quantify the impact of measurement error and chamber protocol on the accuracy and precision of resulting flux estimates, and to develop an efficient calculation scheme for performing such analyses. Measurement errors associated with three different GC systems were characterized and used in the analysis.

Soil Sci. Soc. Am. J. 73:1087-1093

doi:10.2136/sssaj2008.0307

Received 25 Sept. 2008.

*Corresponding author (rod.venterea@ars.usda.gov).

© Soil Science Society of America

677 S. Segoe Rd. Madison WI 53711 USA

All rights reserved. No part of this periodical may be reproduced or transmitted in any form or by any means, electronic or mechanical, including photocopying, recording, or any information storage and retrieval system, without permission in writing from the publisher.

Permission for printing and for reprinting the material contained herein has been obtained by the publisher.

METHODS AND MATERIALS

Simulation of Flux-Chamber N₂O Concentrations

Following Livingston et al. (2006) and Venterea and Baker (2008), chamber trace gas concentration dynamics were modeled using the one-dimensional diffusion-reaction equation in the form:

$$S \frac{\partial C_s}{\partial t} = \frac{\partial}{\partial z} \left(D_p \frac{\partial C_s}{\partial z} \right) + \rho(P-U) \quad [1]$$

where C_s is the soil-gas N₂O concentration (g N m⁻³ gas) as a function of time (t) (h) and depth (z) (m soil), S is a storage coefficient (m³ soil air m⁻³ soil), D_p is the soil-gas diffusion coefficient (m³ gas m⁻¹ soil h⁻¹), ρ is bulk density (g soil m⁻³ soil), and P and U are N₂O production and uptake rates, respectively (g N g⁻¹ soil h⁻¹). Use of Eq. [1] assumes that chamber insertion depth and radius are sufficient to minimize lateral diffusion effects, the chamber is properly sealed and vented, and any gas recirculation system is designed to reduce pressure perturbations (Hutchinson and Livingston, 2002; Xu et al., 2006).

The storage coefficient was defined as

$$S = \varepsilon + K_H \theta \quad [2]$$

where ε is the volumetric air content (m³ gas m⁻³ soil), K_H is the Henry's Law partitioning coefficient (0.698 m³ gas m⁻³ H₂O at 20°C, Wilhelm et al., 1977), and θ is the volumetric water content (m³ H₂O m⁻³ soil) (Venterea and Baker, 2008). Soil-gas diffusivity was calculated using the Rolston and Moldrup (2002) model

$$D_p = D_o \Phi^2 \left(\frac{\varepsilon}{\Phi} \right)^{(2+3/b)} \quad [3]$$

where D_o is the gas diffusivity in free air (0.0497 m² gas h⁻¹ at 20°C, Fuller et al., 1966), Φ is the total porosity (m³ pore space m⁻³ soil), and b is the Campbell pore-size distribution parameter which can be determined from soil-water retention curve data or estimated from soil texture data using the relation in Rolston and Moldrup (2002).

Previous models describing flux chamber gas dynamics have applied Eq. [1] with the assumption that $U = 0$ (Healy et al., 1996; Livingston et al., 2006; Venterea and Baker, 2008). For the current study, we first conducted a preliminary investigation which compared numerical solutions to Eq. [1] with and without the assumption that $U = 0$, using methods described by Venterea and Baker (2008) and Venterea and Stanenas (2008). These simulations indicated that chamber N₂O concentrations are expected to be affected by soil N₂O uptake only under extreme conditions not likely to occur in practice. These conditions included the coexistence of (i) water-filled pore space (WFPS) values less than approximately 65%, (ii) nearly complete anaerobic conditions within the upper 5 cm of soil, (iii) soil N₂O uptake rates higher than most if not all data reported in kinetic studies, and (iv) chamber heights ≤ 10 cm and DTs ≥ 1 h.

The finding that chamber N₂O concentrations are unlikely to be affected by soil uptake processes simplifies accuracy and precision analysis because it justifies the assumption that $U = 0$ in Eq. [1]. Therefore, for subsequent analysis, chamber N₂O concentrations were modeled using an analytical solution to Eq. [1] that is valid under the assumptions that $U = 0$ and that S , D_p and ρ are constants. This solution was derived by Livingston et al. (2006) and is given by

$$C_c(t) = C_c(0) + \frac{f_o \tau}{b} \left[\frac{2}{\sqrt{\pi}} \sqrt{t/\tau} + \exp(t/\tau) \operatorname{erfc}(\sqrt{t/\tau}) - 1 \right] \quad [4]$$

where $C_c(t)$ is the chamber N₂O concentration at time (t) following deployment, $C_c(0)$ is the initial ($t = 0$) N₂O concentration (assumed to be the ambient atmosphere value of 0.371 mg N m⁻³ gas per Solomon et al.,

2007), b is the ratio of internal chamber volume to surface area in contact with soil (i.e., effective chamber height) (m³ gas m⁻² soil), f_o is the steady-state N₂O flux before chamber deployment, the parameter τ is given by $b^2 (S D_p)^{-1}$, and erfc is the complementary error function. The solution represented by Eq. [4] also assumes a homogeneously mixed chamber atmosphere and steady-state soil conditions before chamber deployment.

Generation of Simulated Chamber Data

Application of Eq. [4] to generate simulated chamber time series data requires information regarding (i) soil properties, including bulk density, water content, temperature, and either texture or soil-water retention relationships, (ii) chamber conditions, including effective height (b), total deployment time (DT), and sampling frequency, and (iii) the predeployment flux (f_o). For purposes of demonstration, a model soil having a bulk density of 1.34 Mg m⁻³ and a water content of 0.297 m³ H₂O m⁻³ (equivalent to 60% WFPS) was used. This ρ value represents the mean bulk density over the 0- to 30-cm depth measured by Venterea and Stanenas (2008) in a conventionally tilled soil that was used for previous analysis by Venterea and Baker (2008). A value of 9.6 was used for b based on measurements in these soils by Spaans and Baker (1996), and a temperature of 20°C was assumed for calculating D_o and K_H . The ρ and θ values were used to calculate Φ and ε based on fundamental relations assuming a particle density of 2.65 g cm⁻³, and these values in turn were used to calculate S and D_p using Eq. [2-3]. Simulated chamber data were then generated using Eq. [4] for a range of values for b (5-30 cm), DT (0.3-1.5 h), and f_o (25-1000 $\mu\text{g m}^{-2} \text{h}^{-1}$). Each set of simulated chamber time series data included an initial time 0 sample with either 2 or 4 subsequent sampling events that were equally spaced in time, equivalent to total sampling events of 3 or 5.

Measurement Error Effects

Time series data generated using the procedures described above will predict chamber N₂O concentrations under the condition that concentrations are determined with 100% accuracy. In reality, any method of analysis is imprecise due to fluctuations in sampling techniques and instrument behavior. These variations were incorporated into the modeled time series data using stochastic techniques described below.

Characterization of Measurement Precision

We characterized the precision for three different GC systems that are currently used to analyze N₂O in samples from gas flux chambers. These methods were designed to account for combined sources of imprecision resulting from manual gas sample collection via syringe and transfer of sample from syringe to sealed vial, automated and pressurized transfer of vial contents to the GC, as well as instrument fluctuation. For each system, we collected 20 "samples" of N₂O standard gas contained in pressurized cylinders (Scott Specialty Gases, Plumsteadville, PA). Samples were removed from cylinders via plastic syringe and immediately injected into 9- or 10-mL glass vials sealed with butyl rubber septa in accordance with field chamber sampling techniques (Venterea et al., 2005). The vials were then placed into automated samplers that delivered subsamples of the vial contents to GCs for analysis within 6 h of sample collection.

Gas chromatography systems 1 and 2 each consisted of separate headspace autosamplers (Teledyne Tekmar, Mason, OH, Model 7000/7050) connected to separate GCs (HP/Agilent, Foster City, CA, Model 5890), each equipped with an electron capture detector (ECD) (HP/Agilent) heated to 300°C. The main difference between Systems 1 and 2 was the manufacture date of the ECD (System 1 = 2002, System 2 = 1993). The vials were first pressurized within the autosamplers using helium (He).

During depressurization, the vial contents were directed through 2.0 mL sampling loops before being delivered to the GC carrier gas stream. Both systems used a 1.8-m long \times 3.175-mm od stainless steel Porapak Q 80/100 mesh packed column (Grace, Deerfield, IL) with He carrier gas (20 mL min⁻¹) and a blend of 5% (v/v) methane in 95% (v/v) argon make-up gas (110 mL min⁻¹). Column temperature was held at 55°C until the N₂O peak eluted (1.6 min), at which time column temperature was raised at 70°C min⁻¹ to 100°C and held for 0.5 min. Each system was also equipped with gas drying tubes containing semi-permeable membranes (Perma Pure, Toms River, NJ, MD series) to reduce residual water vapor in the autosampler-to-GC transfer line.

Gas chromatography system 3 consisted of a headspace autosampler (Agilent, Foster City, CA, Model 7694) that was modified by the addition of a diaphragm sample valve (Valco, Houston, TX, Model DV22-2116). Sample vials were initially pressurized within the autosampler using He (138 kPa). After 0.4 min, 60- and 120- μ L sample loops were filled during venting of the pressurized vial. After equilibration (0.4 min), the sample loops were injected onto two different columns within a single GV oven (PerkinElmer, Waltham, Massachusetts, Model Calrus 600). The 60- μ L sample loop was connected to a RT-Molesieve 5A (0.32 mm \times 30 m, Restek, Bellefonte, PA), and the 120 μ L loop to a RT-QSPLOT (0.32 mm \times 30 m, Restek, Bellefonte, PA), each with He carrier gas (2 mL min⁻¹). Both column outlets were connected to a mass spectrometer (PerkinElmer, Waltham, MA, Model 600T) through a diaphragm valve (Valco, Houston, TX, Model DV22-2116) that permitted selection of column effluent stream that was directed to the detector and allowed the oxygen, nitrogen, and water peaks to be safely vented away from the mass spectrometer. Column temperature started at 35°C for 5 min and was raised at 20°C min⁻¹ to 120°C. The N₂O peak eluted from the RT-QSPLOT column at 4.05 min.

The precision of each GC system was determined from replicate analyses of standards ranging in concentration from 0.3 to 10 μ L L⁻¹. For each replicate, raw instrument response (area counts) was converted to concentration using calibration curves derived from the mean responses at each concentration level. For each set of replicates corresponding to each concentration level, the measurement standard deviation (σ) was determined in concentration units (μ L L⁻¹). Coefficients of variation (CV) were calculated from the ratio of σ to the actual standard concentration. Functional relationships between σ and concentration in the form

$$\sigma_i = \alpha_i [1 - \exp(-\beta_i C)] \quad [5]$$

were obtained by nonlinear regression using SigmaPlot (v.10, Systat, Richmond, CA), where the i index refers to GC system 1, 2 or 3, C represents the concentration of the standard gas, and α and β are regression coefficients.

Monte Carlo Analysis

The chamber N₂O concentrations generated by Eq. [4] are referred to as “baseline” time series data, which were used as inputs to Monte Carlo (MC) statistical analyses. Each MC “trial” consisted of adjusting each individual simulated N₂O chamber concentration (C_c), including the initial ($t = 0$) concentration, to account for measurement error by

$$C_c^A = C_c + \zeta \quad [6]$$

where C_c^A is the error-adjusted chamber N₂O concentration and ζ is the measurement error. Each ζ value was randomly selected from a distribution having a mean of 0 and standard deviation σ , which was calculated either as a function of C_c using Eq. [5], or using the relation

$$\sigma = \frac{CV}{100} C_c \quad [7]$$

where CV is expressed as a percentage of the concentration. Equation [7] assumes that σ can be represented as a fixed proportion of the concentration. In both cases, random selections of ζ values from distributions defined by σ were generated by the NormalValue function in the RiskAMP add-in (Structured Data, LLC <http://www.riskamp.com/>) for Microsoft Excel (v. 2002).

Error-adjusted time series data were used to estimate the predeployment flux, which could then be compared with the actual f_o value which was input to Eq. [4]. The estimated flux (f_{est}) was calculated using a linear model and two nonlinear flux schemes. Linear model estimates were obtained by linear regression of C_c^A versus time (t) and calculated from $f_{est} = b C_c^A$ where C_c^A is the slope of C_c^A versus t . A quadratic (Quad) scheme was applied using the LINEST function in Microsoft Excel (v. 2002) to obtain values of coefficients (a , b , and c) in the quadratic function $C_c^A(t) = at^2 + bt - c$ and then calculating $f_{est} = hb$ (Wagner et al., 1997). The model of Hutchinson and Mosier (1981) (“HM model”) was used according to

$$f_{est} = b \ln(\omega) \frac{[C_c^A(\Delta t) - C_c^A(0)]^2}{\Delta t [2C_c^A(\Delta t) - C_c^A(0) - C_c^A(2\Delta t)]} \quad [8]$$

where Δt is the time interval between three sampling events that are equally spaced in time, and where

$$\omega = [C_c^A(\Delta t) - C_c^A(0)] / [C_c^A(2\Delta t) - C_c^A(\Delta t)] \quad [9]$$

A small proportion (<10%) of ω values calculated from the error-adjusted data were less than or equal to 1. For these MC trials, the linear model was used in place of either the HM or Quad schemes, since $\omega \leq 1$ violates a fundamental assumption of these nonlinear models. For the linear and Quad estimates, MC analysis was applied to baseline data consisting of three or five total sampling events during each simulated deployment. The HM model accommodates only three sampling events, equally spaced in time. The percent of relative error (RE) of each flux estimate was calculated as 100% * ($f_{est} - f_o$) / f_o , where a negative RE represents underestimation of f_o (Livingston et al., 2006).

We performed MC “runs” consisting of 1000 individual MC trials, with each trial originating from the same set of baseline time series values. Each run resulted in distributions of 1000 f_{est} values for each of the three flux-calculation schemes, from which the mean, standard deviation, CV, and skewness were calculated. Standard deviation of the f_{est} distributions was assigned the symbol ψ to distinguish it from the measurement standard deviation σ .

We also applied analysis of variance (ANOVA) to results of MC trials. A reference set of baseline chamber N₂O time series values were generated using $f_o = 100 \mu\text{g N m}^{-2} \text{h}^{-1}$. Five separate sets of baseline time series data were also generated using f_o values of 75, 80, 85, 90, and 92.5 $\mu\text{g N m}^{-2} \text{h}^{-1}$. These simulations all assumed that $h = 15$ cm and $DT = 1$ h. Monte Carlo trials were then used to generate multiple sets of error-adjusted time series data using the reference baseline data and each of the five levels of comparison baseline data. Flux estimates (i.e., f_{est} values) calculated using the error-adjusted reference data (i.e., where $f_o = 100 \mu\text{g N m}^{-2} \text{h}^{-1}$) were then compared to the f_{est} values calculated from the error-adjusted comparison data, one level at a time for each value of f_o ranging from 75 to 92.5 $\mu\text{g N m}^{-2} \text{h}^{-1}$. The f_{est} values calculated from the first two MC trials for the reference and comparison set were compared using ANOVA with $n = 2$. If a P value ≥ 0.05 was found, additional MC trial-generated f_{est} values were included in the ANOVA (with $n > 2$) until a significant difference ($P < 0.05$) was found. The sequence of f_{est} values selected for comparison was determined randomly using the RiskAMP NormalValue function. This entire procedure was repeated five times, each using independent sets of MC-generated

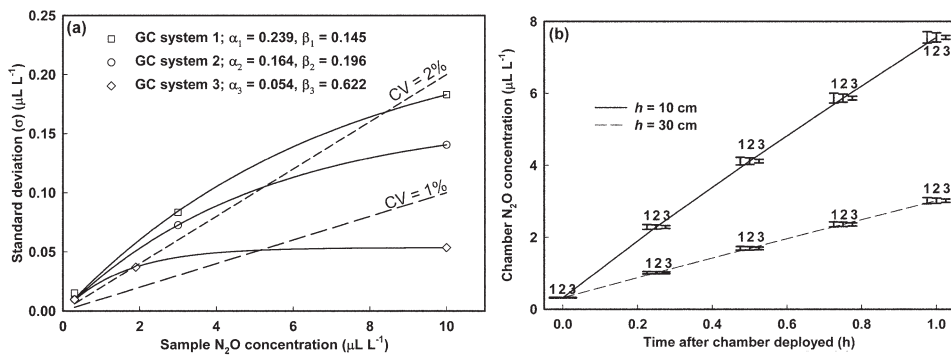


Fig. 1. (a) Measurement standard deviation (σ) versus nitrous oxide (N_2O) concentration for GC systems 1, 2, and 3 where solid lines are lines of best fit using Eq. [5], dashed lines are hypothetical cases of constant coefficient of variation (CV), and α and β values relate to Eq. [5], and (b) simulated chamber N_2O concentrations versus time after chamber deployed calculated from Eq. [4] with effective chamber heights (h) of 10 and 30 cm and predeployment flux (f_o) of $1000 \mu\text{g N m}^{-2} \text{h}^{-1}$, where bars indicate standard deviations for each GC system (horizontal positions of bars 1 and 3 are offset slightly to aid viewing).

errors. The mean number of MC trials required to achieve $P < 0.05$ was calculated for each comparison level. P values were determined by ANOVA with least significant differences means comparisons using Statgraphics (v. 5.1, Manugistics, Rockville, MD).

RESULTS AND DISCUSSION

Measurement standard deviation (σ) increased with concentration and was well-described by Eq. [5] for all three GC systems (Fig. 1a). Coefficient of variation values ranged from 3.2 to 5.1% at $0.3 \mu\text{L L}^{-1}$ and from 0.5 to 1.8% at the highest concentration ($10 \mu\text{L L}^{-1}$). System 3, which used a mass spectrometer detector, had lower variances ($\text{CV} = 0.5\text{--}3.2\%$) compared with the two ECD detector systems ($\text{CV} = 1.4\text{--}5.1\%$). Arnold et al. (2001) similarly found that CVs for N_2O analysis by GC/ECD with autosampler injection decreased from 5.6 to 13.6% for ambient-level

concentrations to 1.7 to 2.0% for N_2O levels above $1 \mu\text{L L}^{-1}$. Lower CV values (1–2%) using GC/ECD with manual injection for ambient-level analysis have been reported (Arnold et al., 2001; Matthias et al., 1993). This suggests, not surprisingly, that vial pressurization and automated sample injection introduces additional sources of variability compared with manual injection. Results reported by Arnold et al. (2001) suggest that CV values for manual injection may be relatively constant across concentration, which is equivalent to a straight line relation between concentration and standard deviation, as expressed in Eq. [7] and as shown by the dashed lines in Fig. 1a. The manual injection data in Arnold et al. (2001) are not conclusive on this point, and to our knowledge similar information has not been reported elsewhere. The case of a constant CV is considered here as a hypothetical case.

Chamber time series data simulated by Eq. [4] are shown in Fig. 1b with error bars representing σ calculated from Eq. [5]. Baseline chamber data such as that in Fig. 1b were used in MC trials to generate error-adjusted time series N_2O concentrations, which were then used to calculate f_{est} using each FC scheme. The results of multiple MC runs, each consisting of 1000 individual MC trials, are shown for $f_o = 1000$ (Fig. 2a and 3a) and $f_o = 100 \mu\text{g N m}^{-2} \text{h}^{-1}$ (Fig. 2b and 3b). The solid symbols in Fig. 2 and 3 represent the f_{est} values calculated from the baseline chamber data assuming no measurement error. The open symbols and error bars in Fig. 2 and 3 represent means and standard deviations (ψ), respectively, of f_{est} distributions resulting from 1000 MC trials. Figure 2 assumes the σ versus C_C relationship obtained for GC system 1 per Eq. [5], and Fig. 3 assumes that measurement error can be represented as a constant $\text{CV} = 1.5\%$ per Eq. [7].

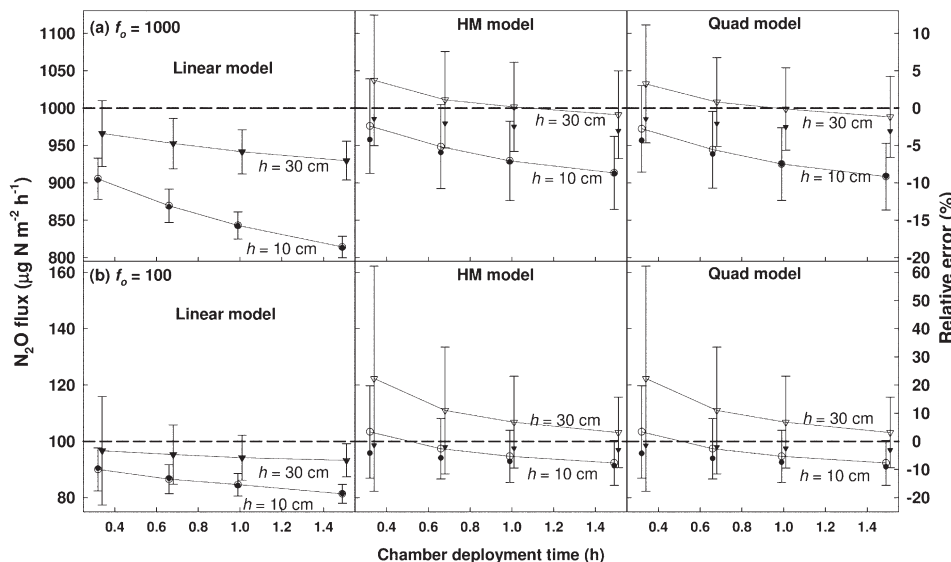


Fig. 2. Estimated N_2O flux (f_{est} , left axis) and relative error (RE, right axis) calculated using Linear, HM, and Quad schemes versus deployment time with effective chamber heights (h) of 10 (circles) and 30 cm (triangles) and with predeployment fluxes (f_o) of (a) 1000 and (b) $100 \mu\text{g N m}^{-2} \text{h}^{-1}$. Open symbols and error bars represent means and standard deviations (ψ), respectively, of flux-estimate distributions resulting from 1000 Monte Carlo trials assuming measurement error for GC system 1. Solid symbols represent f_{est} calculated from baseline chamber data assuming no measurement error (open and closed symbols are indistinguishable in some cases). Baseline chamber N_2O concentrations were simulated using Eq. [4] with three sampling events. Dashed lines represent f_o .

concentrations to 1.7 to 2.0% for N_2O levels above $1 \mu\text{L L}^{-1}$. Lower CV values (1–2%) using GC/ECD with manual injection for ambient-level analysis have been reported (Arnold et al., 2001; Matthias et al., 1993). This suggests, not surprisingly, that vial pressurization and automated sample injection introduces additional sources of variability compared with manual injection. Results reported by Arnold et al. (2001) suggest that CV values for manual injection may be relatively constant across concentration, which is equivalent to a straight line relation between concentration and standard deviation, as expressed in Eq. [7] and as shown by the dashed lines in Fig. 1a. The manual injection data in Arnold et al. (2001) are not conclusive on this point, and to our knowledge similar information has not been reported elsewhere. The case of a constant CV is considered here as a hypothetical case.

Chamber time series data simulated by Eq. [4] are shown in Fig. 1b with error bars representing σ calculated from Eq. [5]. Baseline chamber data such as that in Fig. 1b were used in MC trials to generate error-adjusted time series N_2O concentrations, which were then used to calculate f_{est} using each FC scheme. The results of multiple MC runs, each consisting of 1000 individual MC trials, are shown for $f_o = 1000$ (Fig. 2a and 3a) and $f_o = 100 \mu\text{g N m}^{-2} \text{h}^{-1}$ (Fig. 2b and 3b). The solid symbols in Fig. 2 and 3 represent the f_{est} values calculated from the baseline chamber data assuming no measurement error. The open symbols and error bars in Fig. 2 and 3 represent means and standard deviations (ψ), respectively, of f_{est} distributions resulting from 1000 MC trials. Figure 2 assumes the σ versus C_C relationship obtained for GC system 1 per Eq. [5], and Fig. 3 assumes that measurement error can be represented as a constant $\text{CV} = 1.5\%$ per Eq. [7].

Results in Fig. 2 and 3 demonstrate the inherent trade-offs between accuracy and precision of chamber-based N_2O flux estimates. As previously shown by Livingston et al. (2006) and Venterea and Baker (2008), flux estimates based on the assumption of zero measurement error are increasingly accurate for increasing h and decreasing DT, and also for nonlinear compared with linear FC schemes. These trends are reflected in the solid symbols in Fig. 2 and 3 which converge toward $f_{est} = f_o$ and $\text{RE} = 0$ for increasing h , decreasing DT, and for the nonlinear FC schemes. Thus, an apparent approach to improve the accuracy of

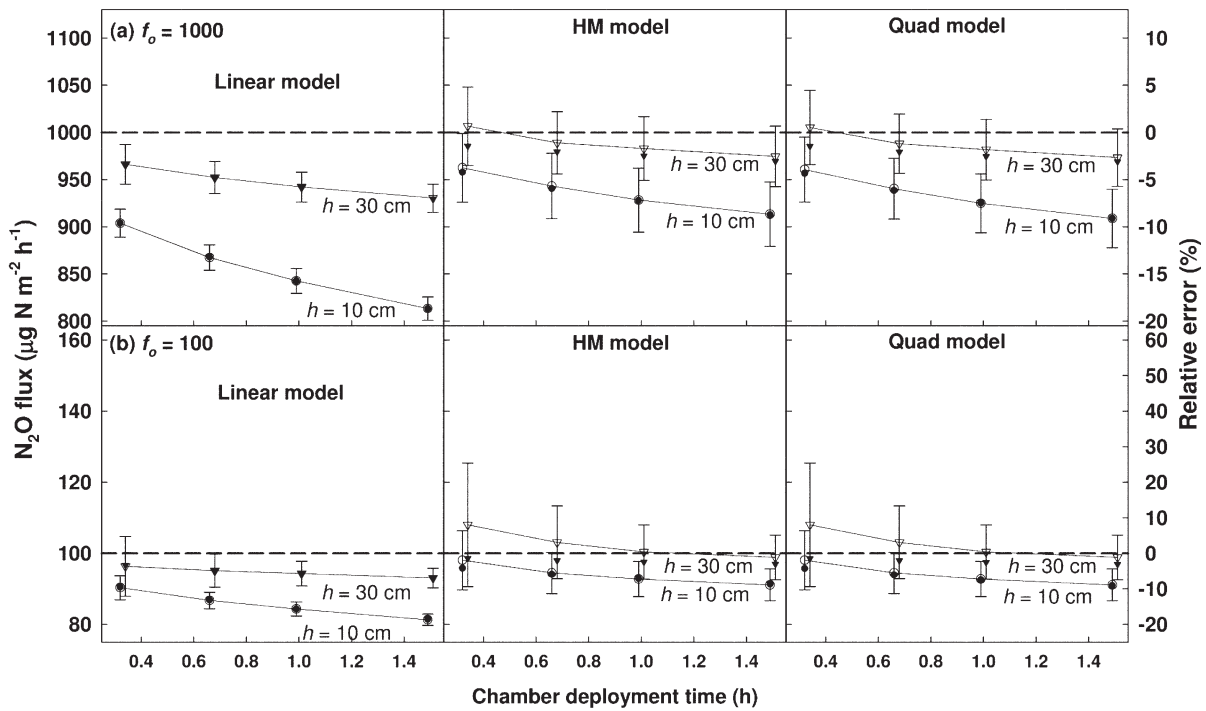


Fig. 3. Estimated N_2O flux (f_{est} , left axis) and relative error (RE, right axis) calculated using Linear, HM, and Quad schemes versus deployment time with effective chamber heights (h) of 10 (circles) and 30 cm (triangles) and with predeployment fluxes (f_o) of (a) 1000 and (b) 100 $\mu\text{g N m}^{-2} \text{h}^{-1}$. Open symbols and error bars represent means and standard deviations (σ), respectively, measurement error can be represented by constant $CV=1.5\%$. Solid symbols represent f_{est} calculated from baseline chamber data assuming no measurement error (open and closed symbols are indistinguishable in some cases). Baseline chamber N_2O concentrations were simulated using Eq. [4] with 3 sampling events. Dashed lines represent f_o .

flux estimates would be to use taller chambers, shorter DTs, and/or a nonlinear scheme. However, as illustrated by the error bars in Fig. 2 and 3, each of these approaches also results in increased variability. The shortest DTs (0.33 h) and largest h values (30 cm) resulted in standard deviations in flux estimates (ψ) more than twice as large in some cases as compared to longer DTs and shorter h values. As expected, the magnitude of these effects was greater for errors generated by GC system 1 (Fig. 2) compared to the hypothetical case of a constant CV of 1.5% (Fig. 3).

Venterea and Baker (2008) previously showed that the accuracy of flux estimates (expressed as RE) was independent of the predeployment (f_o). In contrast, the current results show that the precision of flux estimates is highly sensitive to f_o . The magnitude of variation relative to the flux increased substantially as f_o decreased from 1000 to 100 $\text{g N m}^{-2} \text{h}^{-1}$ as indicated by comparing Fig. 2a to 2b and Fig. 3a to 3b. The effect of flux on variability is illustrated more directly in Fig. 4 which shows that flux-estimate CV increased exponentially as f_o decreased. For the conditions examined in Fig. 4, CVs ranged up to 30% for the linear model and 75% for nonlinear schemes. The flux-estimate CVs in Fig. 4 compare to measurement CVs of 0.5 to 5.1% in Fig. 1. Thus, measurement variance (σ) was effectively magnified into a much larger flux-estimate variance (ψ), particularly for nonlinear schemes. It is important to note that these CVs represent variances in estimated fluxes under the condition of a constant predeployment flux (f_o).

Results in Fig. 2 and 3 also show that the mean flux estimates using stochastically adjusted time series data (open symbols) coincided nearly identically with estimates that assume no measurement error (solid symbols) for the linear flux model. However, this was not consistently the case for nonlinear schemes, which tended to generate higher mean flux estimates when measurement error

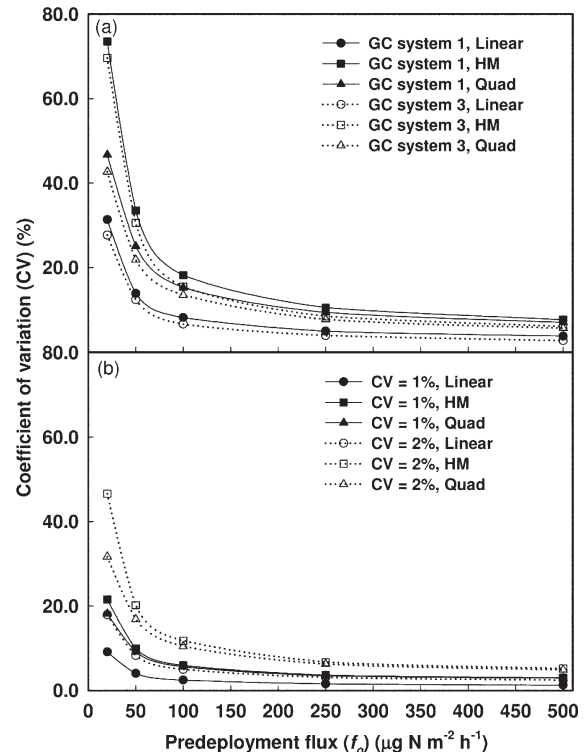


Fig. 4. Coefficients of variation (CV) of N_2O flux estimates at varying predeployment flux (f_o), using the linear, HM and Quad flux-calculation schemes assuming measurement standard deviation for (a) GC system 1 (solid lines) and 3 (dotted lines), and (b) constant CVs of 1% (solid lines) and 2% (dotted lines). Each value is calculated from a distribution generated by 1000 Monte Carlo trials using baseline chamber N_2O time series data calculated by Eq. [4] with deployment time of 0.67 h, effective chamber height of 20 cm, with three sampling events.

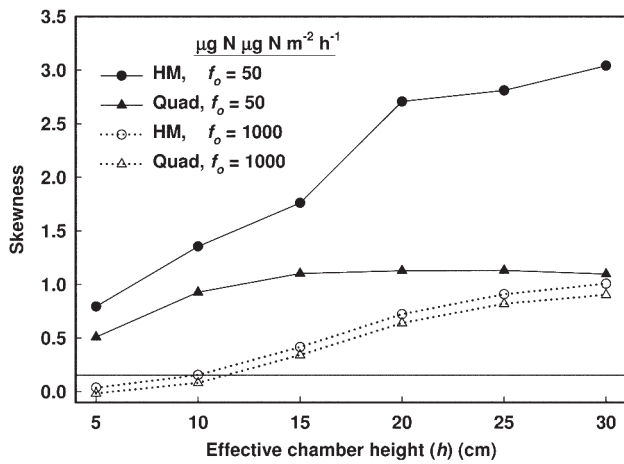


Fig. 5. Skewness of N_2O flux distributions calculated from the HM and Quad schemes at varying effective chamber height (h) and predeployment flux (f_o). Each value represents the mean skewness of 10 distributions, each generated by 1000 Monte Carlo trials assuming measurement standard deviation of GC system 3 using baseline chamber N_2O time series data calculated using Eq. [4] with deployment time of 0.67 h and three sampling events. The horizontal line corresponds to the value $2 = 0.155$ where is given by Eq. [10].

was considered. Additional analysis indicated that f_{est} distributions generated by the HM and Quad schemes were positively skewed. Like the variance, skewness increased with increasing h and decreasing f_o (Fig. 5) as well as decreasing DT (not shown). Some of the skewness resulted from substitution of the linear model for cases where $\omega \leq 1$ (Eq. [9]), due to the fact that the linear model generates higher flux estimates than either nonlinear scheme when $\omega < 1$. When these substitutions were not made, skewness in the Quad-generated distributions was eliminated. However, the HM-generated distributions were inherently skewed in the absence of the linear substitution. Skewness values were also compared with the “standard error of the skewness” given by

$$\kappa = \sqrt{\frac{6n(n-1)}{(n-2)(n+1)(n+3)}} \quad [10]$$

where $n = 1000$. Skewness values exceeding approximately $2\kappa = 0.155$ are considered to be significantly skewed (Matalas and Benson, 1968). For most of the conditions evaluated in Fig. 5, skewness exceeded this criterion.

The variance and skewness effects described above will decrease confidence in N_2O flux estimates and inhibit the detection of differences due to experimental or environmental factors. The ANOVA results indicate that the linear FC scheme was much more sensitive to detecting differences in flux as measured by the number of MC trials required to achieve a statistically significant difference (Fig. 6). The Quad scheme showed slightly better sensitivity than the HM scheme. Increasing the number of sampling events from 3 to 5 during the same 1-h deployment period improved the sensitivity for the Linear and Quad schemes.

CONCLUSIONS

Using gas transport theory and MC analysis, this study demonstrated that clear trade-offs exist between accuracy and precision in determining N_2O fluxes using chambers. One obvious conclusion is that characterization of measurement error inherent to any sampling and analytical protocol, such as that shown in Fig. 1a, is critical to any assessment of chamber method reliability. A linear FC scheme was shown to be more sensitive to detecting relative differences among chamber locations than nonlinear models. This result leads to the recommendation (which is made with some caution) that, in cases where the primary objective is to determine relative differences in N_2O emissions arising from experimental factors, the linear scheme with longer deployment times and shorter chambers will be more statistically robust. However, actual predeployment fluxes will be underestimated to a greater extent than with nonlinear schemes. Thus, there is the danger that published emissions data based on a linear model would be subsequently used for making assessments on an absolute scale, for example, in national or global emissions inventories. It is therefore also recommended that some accuracy analysis be included with flux data, regardless of the calculation scheme employed. This can only serve to improve the absolute accuracy of N_2O emissions inventories.

An additional caveat is required for the case where the experimental factors being examined result in substantially different bulk density or water content among treatments, for example resulting from tillage or organic amendments. As shown by Venterea and Baker (2008), soil profiles with higher air-filled porosity will generate more nonlinearity in chamber data. In this case, and in any case where accurate determination of the predeployment flux is of highest priority, shorter deployment times, larger chambers, and/or nonlinear flux models is recommended. Since the Quad model performed the same or better than the HM model in terms of accuracy, precision, and skewness, the Quad model would be recommended.

Especially when nonlinear flux schemes are used, evaluation of both accuracy and precision using the type of analysis done here is recommended so that the most favorable balance can be achieved. To expedite this analysis, we developed a spreadsheet-based tool which calculates relative errors and variances, and also expedites ANOVA comparisons (e.g., Fig. 6), for specified soil and measurement conditions. This spreadsheet and user informa-

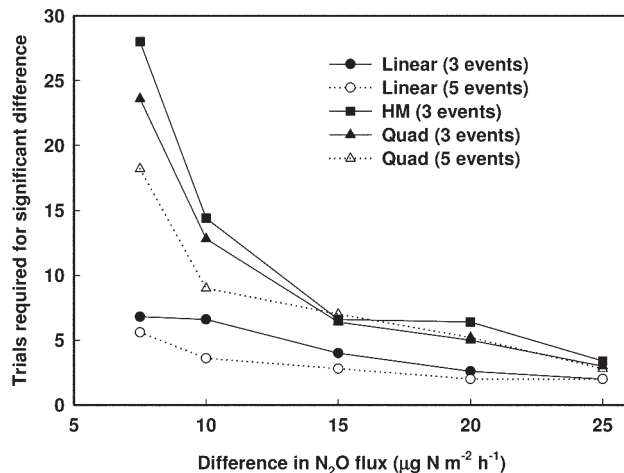


Fig. 6. Number of Monte Carlo trials required to achieve a significant difference ($P < 0.05$) in fluxes calculated using the Linear, HM, and Quad models versus the difference in predeployment flux (f_o), assuming measurement standard deviation of GC system 1 with either three (solid lines, closed symbols) or five sampling events (dotted lines, open symbols). Each point represents the mean number of Monte Carlo trials based on five independent comparisons. Baseline chamber N_2O concentrations were calculated from Eq. [4] with reference $f_o = 100 \mu g N m^{-2} h^{-1}$, effective chamber height = 15 cm, and deployment time = 1 h

tion are available on-line at <http://www.ars.usda.gov/pandp/people/people.htm?personid=31831> or from the authors on request. One assumption of the spreadsheet-based analysis is that the soil is vertically uniform with respect to physical properties. In reality, soils are rarely uniform. However, as suggested by Venterea and Baker (2008) a conservative estimate of accuracy can be obtained by assuming near-surface bulk density and water content values. If detailed data regarding bulk density and water content variation with depth are available, more precise analysis can be obtained using numerical techniques (Venterea and Baker, 2008).

Ultimately, the accuracy-precision dilemma will be overcome when high-precision analytical instruments become available for N₂O that allow for chamber deployment times of <0.25 h, analogous to instruments commonly used for soil respiration (Davidson et al., 2002). Tunable diode laser spectrometers (TDLS) used for micrometeorological flux measurements can achieve high-precision analysis of near-ambient N₂O levels (Wagner-Riddle et al., 2007), although high expense and lack of portability inhibits their widespread use for chambers. Photoacoustic detectors (PADs) are seeing some application for short-duration chamber-based N₂O fluxes (e.g., Flechard et al., 2005). However, ambient-level precision of a PAD reported by Flechard et al. (2005) was no better than the GC systems evaluated here (i.e., CV = 6.25%).

ACKNOWLEDGMENTS

This work was improved based on the suggestions of three anonymous reviewers, and was supported by the USDA Agricultural Research Service (ARS) under the ARS GRACEnet Project.

REFERENCES

- Arnold, S.L., T.B. Parkin, J.W. Doran, B. Eghball, and A. Mosier. 2001. Automated gas sampling system for laboratory analysis of CH₄ and N₂O. *Commun. Soil Sci. Plant Anal.* 32:2795–2807.
- Crutzen, P.J., A.R. Mosier, K.A. Smith, and W. Winiwarter. 2008. N₂O release from agro-biofuel production negates global warming reduction by replacing fossil fuels. *Atmos. Chem. Phys.* 8:389–395.
- Davidson, E.A., K. Savage, L.V. Verchot, and Rosa Navarro. 2002. Minimizing artifacts and biases in chamber-based measurements of soil respiration. *Agric. For. Meteorol.* 113:21–37.
- Denman, K.L., G. Brasseur, A. Chidthaisong, R. Ciais, P.M. Cox, R.E. Dickinson, D. Hauglustaine, C. Heinze, E. Holland, D. Jacob, U. Lohmann, S. Ramachandran, P.L. da Silva Dias, S.C. Wofsy, and X. Zhang. 2007. Couplings between changes in the climate system and biogeochemistry, p. 499–587. *In* S. Solomon et al. (ed.) *Climate change 2007: The physical science basis. Contribution of Working Group I to the Fourth Assessment Report of the Intergovernmental Panel on Climate Change*. Cambridge Univ. Press, New York, NY.
- Flechard, C.R., A. Neftel, M. Jocher, C. Amman, and J. Fuhrer. 2005. Bi-directional soil/atmosphere N₂O exchange over two mown grassland systems with contrasting management practices. *Glob. Change Biol.* 11:2114–2127.
- Forster, P., V. Ramaswamy, P. Artaxo, T. Bernsten, R. Betts, D.W. Fahey, J. Haywood, J. Lean, D.C. Lowe, G. Myhre, J. Nganga, R. Prinn, G. Raga, M. Schulz, and R. Van Dorland. 2007. Changes in atmospheric constituents and in radiative forcing, p. 129–234. *In* S. Solomon et al. (ed.) *Climate change 2007: The physical science basis. Contribution of Working Group I to the Fourth Assessment Report of the Intergovernmental Panel on Climate Change*. Cambridge Univ. Press, New York, NY.
- Fuller, E.N., P.D. Schettler, and J.C. Giddings. 1966. A new method for prediction of binary gas-phase diffusion coefficients. *Ind. Eng. Chem.* 58:19–27.
- Healy, R.W., R.G. Striegl, T.F. Russell, G.L. Hutchinson, and G.P. Livingston. 1996. Numerical evaluation of static-chamber measurements of soil-atmosphere gas exchange: Identification of physical processes. *Soil Sci. Soc. Am. J.* 60:740–747.
- Hutchinson, G.L., and G.P. Livingston. 2002. Soil-atmosphere gas exchange, p. 1159–1182. *In* J.H. Dane and G.C. Topp (ed.) *Methods of soil analysis. Part 4. SSSA Book Ser. 5. SSSA, Madison, WI.*
- Hutchinson, G.L., and A.R. Mosier. 1981. Improved soil cover method for field measurement of nitrous oxide fluxes. *Soil Sci. Soc. Am. J.* 45:311–316.
- Livingston, G.P., and G.L. Hutchinson. 1995. Enclosure-based measurement of trace gas exchange: Applications and sources of error, p. 164–205. *In* P.A. Matson and R.C. Harriss (ed.) *Biogenic trace complexes. 2nd ed. Spec. Publ. No. 17. Blackwell Science Ltd., Oxford, UK.*
- Livingston, G.P., G.L. Hutchinson, and K. Spartalian. 2006. Trace gas emission in chambers: A non-steady-state diffusion model. *Soil Sci. Soc. Am. J.* 70:1459–1469.
- Matalas, N.C., and M.A. Benson. 1968. Note on the standard error of the coefficient of skewness. *Water Resour. Res.* 4:204–205.
- Matthias, A.D., J.F. Artiola, and S.A. Musil. 1993. Preliminary study of N₂O flux over irrigated Bermuda grass in a desert environment. *Agric. For. Meteorol.* 64:29–45.
- Mosier, A.R., A.D. Halvorson, G.A. Peterson, G.P. Robertson, and L. Sherrerd. 2005. Measurement of net global warming potential in three agroecosystems. *Nutrient Cycling Agroecosystems* 72:67–76.
- Robertson, G.P., E.A. Paul, and R.R. Harwood. 2000. Greenhouse gases in intensive agriculture: Contributions of individual gases to the radiative forcing of the atmosphere. *Science* 289:1922–1925.
- Rochette, P., and N.S. Eriksen-Hamel. 2008. Chamber measurements of soil nitrous oxide flux: Are absolute values reliable? *Soil Sci. Soc. Am. J.* 72:331–342.
- Rolston, D.E., and P. Moldrup. 2002. Gas diffusivity, p. 1113–1139. *In* J.H. Dane and G.C. Topp (ed.) *Methods of soil analysis. Part 4. SSSA Book Ser. 5. SSSA, Madison, WI.*
- Solomon, S., D. Qin, M. Manning, R.B. Alley, T. Bernsten, N.L. Bindoff, Z. Chen, A. Chidthaisong, J.M. Gregory, G.C. Hegerl, M. Heimann, B. Hewitson, B.J. Hoskins, F. Joos, J. Jouzel, V. Kattsov, U. Lohmann, T. Matsuno, M. Molina, N. Nicholls, J. Overpeck, G. Raga, V. Ramaswamy, J. Ren, M. Rusticucci, R. Somerville, T.F. Stocker, P. Whetton, R.A. Wood, and D. Wratt. 2007. Technical summary, p. 19–91. *In* S. Solomon et al. (ed.) *Climate change 2007: The physical science basis. Contribution of Working Group I to the Fourth Assessment Report of the Intergovernmental Panel on Climate Change*. Cambridge Univ. Press, New York, NY.
- Spaans, E.J., and J.M. Baker. 1996. The soil freezing characteristic: Its measurement and similarity to the soil moisture characteristic. *Soil Sci. Soc. Am. J.* 60:13–19.
- Stehfest, E., and L. Bouwman. 2006. N₂O and NO emission from agricultural fields and soils under natural vegetation: Summarizing available measurement data and modeling of global annual emissions. *Nutr. Cycling Agroecosyst.* 74:207–228.
- Venterea, R.T., M. Burger, and K.A. Spokas. 2005. Nitrogen oxide and methane emissions under varying tillage and fertilizer management. *J. Environ. Qual.* 34:1467–1477.
- Venterea, R.T., and A.J. Stanenas. 2008. Profile analysis and modeling of reduced tillage effects on soil nitrous oxide flux. *J. Environ. Qual.* 37:1360–1367.
- Venterea, R.T., and J.M. Baker. 2008. Effects of soil physical nonuniformity on chamber-based gas flux estimates. *Soil Sci. Soc. Am. J.* 72:1410–1417.
- Verge, X.P.C., C. De Kimpe, and R.L. Desjardins. 2007. Agricultural production, greenhouse gas emissions and mitigation potential. *Agric. For. Meteorol.* 142:255–269.
- Wagner, S.W., D.C. Reicosky, and R.S. Alessi. 1997. Regression models for calculating gas fluxes measured with a closed chamber. *Agron. J.* 89:279–284.
- Wagner-Riddle, C., A. Furon, N.L. McLaughlin, I. Lee, J. Barbeau, S. Jayasundara, G. Parkin, P. Von Bertoldi, and J. Warland. 2007. Intensive measurement of nitrous oxide emissions from a corn–soybean–wheat rotation under two contrasting management systems over 5 years. *Glob. Change Biol.* 13:1722–1736.
- Wilhelm, E., R. Battino, and R.J. Wilcock. 1977. Low-pressure solubility of gases in water. *Chem. Rev.* 77:219–262.
- Xu, L., M.D. Furtaw, R.A. Madsen, R.L. Garcia, D.J. Anderson, and D.K. McDermitt. 2006. On maintaining pressure equilibrium between a soil CO₂ flux chamber and the ambient air. *J. Geophys. Res. Atm.* 111: doi:10.1029/2005JD006435.